Chemical Engineering Journal 148 (2009) 354–364

Contents lists available at ScienceDirect

Chemical Engineering Journal

journal homepage: www.elsevier.com/locate/cej

Kinetic study and equilibrium isotherm analysis of Congo Red adsorption by clay materials

Vipasiri Vimonses[a,b], Shaomin Lei[c], Bo Jin[a,b,d,*], Chris W.K. Chow[d], Chris Saint[b,d]

[a] School of Chemical Engineering, The University of Adelaide, Adelaide, SA 5005, Australia
[b] School of Earth and Environmental Sciences, The University of Adelaide, Adelaide, SA 5005, Australia
[c] School of Resource and Environment Engineering, Wuhan University of Technology, Wuhan 430070, China
[d] Australian Water Quality Centre, SA Water Corporation, Bolivar, SA 5108, Australia

ARTICLE INFO

Article history:
Received 3 June 2008
Received in revised form 20 August 2008
Accepted 9 September 2008

Keywords:
Adsorption
Sodium bentonite
Kaolin
Zeolite
Congo Red

ABSTRACT

This study was to evaluate the adsorption capability of clay minerals of bentonite, kaolin and zeolite to remove Congo Red from aqueous solution. The experiments were carried out in a batch system to optimise operation variables: adsorbent dosage, Congo Red concentration, pH and temperature. Adsorption kinetic and equilibrium isotherm of the clay materials were studied using pseudo-first order and second order kinetic equations, and Freundlich and Langmuir models. The equilibrium data of kaolin was found to best fit to the Langmuir model, while bentonite and zeolite were best explained by the Freundlich model. The adsorption kinetic followed the pseudo-second order equation for the three adsorbents. Intra-particle diffusion studies revealed that the adsorption rates were not solely controlled by the diffusion step. Further thermodynamic investigations showed that the adsorption is an exothermic and spontaneous process. Sodium bentonite demonstrated the best adsorptive capacity followed by kaolin clay, and they can be employed as low-cost alternatives for recalcitrant dye removal from industrial wastewater.

1. Introduction

The treatment of effluent containing dyestuff poses considerable problems in the wastewater industry. Synthetic dyes are one of the most common pollutants which are frequently found in dye manufacturing and textile finishing production. The removal of these dyes from water bodies is extremely important from an environmental point of view. Even very low concentration of the dyes present in water can be highly toxic to aquatic systems [1]. The high stability and toxicity are the major problem in the treatment of wastewater containing dyes. In addition, dyes are resistant to light and moderate oxidative agents; therefore, they cannot be completely removed by conventional biological treatment processes, such as activated sludge and anaerobic digestion.

A number of technologies have been developed and used for removal of the dye contaminants from wastewater; including adsorption, coagulation/flocculation, advanced oxidation processes, ozonation, membrane filtration and biological treatment [2]. Adsorption has been recognised as the most popular treatment process for the removal of the dyes in aqueous solution with the advantages of high efficiency, simple operation, and easy recovery and reuse of adsorbent. Activated carbon adsorption shows high effectiveness in removal of organic and inorganic pollutants, including dyes and pigments. However, the use of this adsorbent in wastewater treatment is still limited because of its high cost and difficulty in regeneration. Many alternative adsorbent materials have been studied to remove dyes from water, including activated carbon from cheap carbon source [3,4], fly ash [5], orange peel [6], waste red mud [7] and clay minerals [8], etc.

The use of clay materials over commercially available adsorbents is becoming popular due to their low-cost, abundant availability, non-toxicity and potential for ion exchange. A number of clay materials: sepiolite [9], kaolinite [10], montmorillonite [11], smectite [12], bentonite [13] and zeolite [14] have been investigated for removal of dyes. These clay minerals are of interest according to their variety of structural and surface properties, high chemical stability, high specific surface area and high adsorption capacity [15].

Congo Red (CR) [1-naphthalenesulfonic acid, 3,3′-(4,4′-biphenylenebis (azo)) bis(4-amino-)disodium salt] is a benzidine-based anionic diazo dye prepared by coupling tetrazotised benzidine with two molecules of napthionic acid [3]. The molecular structure of CR is illustrated in Fig. 1. In this present work, CR is chosen as an anionic dye surrogate indicator due to its chemical composition and environmental concern. Effluent containing CR is produced from

* Corresponding author at: School of Chemical Engineering, The University of Adelaide, Adelaide, SA 5005, Australia. Tel.: +61 8 8303 7056; fax: +61 8 8303 6222.
E-mail address: bo.jin@adelaide.edu.au (B. Jin).

1385-8947/$ – see front matter © 2008 Published by Elsevier B.V.
doi:10.1016/j.cej.2008.09.009

Nomenclature

C_i	initial dye concentration of dye solution (mg l^{-1})
C_e	concentration of dye solution at adsorption equilibrium (mg l^{-1})
ΔG°	Gibbs free energy (kJ mol^{-1})
h	initial adsorption rate of pseudo-second order model (mg g^{-1} min^{-1})
ΔH°	enthalpy (kJ mol^{-1})
k_{id}	intra-particle diffusion rate constant (mg g^{-1} min^{-1})
k_1	Pseudo-first order rate constant (min^{-1})
k_2	Pseudo-second order rate constant (g mg^{-1} min^{-1})
K_C	adsorption equilibrium constant
K_F	Freundlich constants related to adsorption capacity (mg$^{1-1/n}$ l$^{1/n}$ g^{-1})
K_L	Langmuir constant (l mg^{-1}).
m	weight of the adsorbents (g)
n	Freundlich isotherm constant related to adsorption intensity
q_e	equilibrium adsorption capacity of adsorbent (mg g^{-1})
q_{ec}	equilibrium capacity obtained from dynamic model (mg g^{-1}).
q_{ee}	equilibrium capacity of the adsorbent obtained from experiment (mg g^{-1})
q_m	monolayer adsorption capacity of adsorbent (mg g^{-1})
q_t	amount of dye adsorbed per unit of adsorbent at time t (mg g^{-1})
r^2	linear correlation coefficient
R	ideal gas constant (8.314 J mol^{-1} K^{-1})
R_L	dimensionless separation factor
ΔS°	entropy (J mol^{-1} K^{-1})
t	contact time (min)
χ^2	Chi-square error function

textiles, printing, dyeing, paper, and plastic industries [3,16]. This anionic dye can be metabolised to benzidine, a known human carcinogen [17]. Yet, the treatment of CR contaminated wastewater can be complicated due to its complex aromatic structure, providing the dye physicochemical, thermal and optical stability, and resistance to biodegradation and photodegradation.

The objective of this study is to evaluate the adsorption capacity of locally available clay materials (i.e. sodium bentonite, kaolin clay and zeolite) to remove CR from water. The research focused on evaluating how the process operation parameters of initial dye concentration, adsorbent dosage, pH and temperature affect the adsorption capacity of the Australian clay minerals. The best-fit equilibrium isotherms were determined by Freundlich and Langmuir models. Adsorption kinetic models were employed to analyse the kinetics and mechanisms of CR adsorption on the adsorbents.

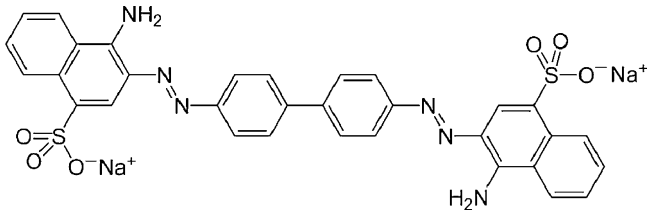

Fig. 1. Molecular structure of Congo Red.

Table 1
Physical and chemical properties of Australian clay materials.

Chemical compound (%)	Natural adsorbents		
	Sodium bentonite	Kaolin	Zeolite
SiO_2	56.0	48.7	68.26
Al_2O_3	16	34.6	12.99
Fe_2O_3	4.6	0.9	1.37
CaO	0.9	0.1	2.09
K_2O	0.4	1.2	4.11
TiO_2		1.3	0.23
MnO			0.06
MgO	3.3	0.4	0.83
Na_2O	2.9	0.2	0.64
P_2O_5			0.06
H_2O	10.0		
LOI	5.7	12.1	8.87
CEC	95 meq/100 g		120 meq/100 g
Particle size	D_{85}75 μm	D_{99}38 μm	D_{100}70 μm
Density	1.0 g cm^{-3}	0.6 g cm^{-3}	1.1–1.6 g cm^{-3}
Specific surface area	25.70 m^2 g^{-1}	20.28 m^2 g^{-1}	8.31 m^2 g^{-1}

Thermodynamics were also applied to examine adsorptive tendency of these materials.

2. Materials and methods

2.1. Materials

Three Australian clay minerals, sodium bentonite, kaolin and zeolite, were employed to study their dye adsorption capacity to remove CR. Sodium bentonite with high montmorillonite and dry milled white kaolin clay were obtained from Unimin Australia Ltd, and Escott zeolite was provided by Zeolite Australia Ltd. This zeolite contains clinoptilolite as the main crystalline component. Physico-chemical properties of each material are given in Table 1. All materials were used as received without other treatment apart from drying at 100 °C for 1 h to remove excess moisture, and then kept in a desiccator until analysed. Congo Red ($C_{32}H_{22}N_6Na_2O_6S_2$, Labchem Ajax Finechem Australia) was used as received. The dye solution was prepared to the desired concentrations using Milli-Q water.

2.2. Characterisation of surface properties of clay materials

The specific surface area of the mineral samples was measured using Brunauer–Emmet–Teller (BET) method. Results were obtained by means of pure liquid N_2 adsorption at 77 ± 0.5 K using a Gemini V2.00 surface analyser (Micromeritics, USA). Prior to analysis, all samples were degassed under vacuum at 105 °C for 12 h.

X-ray diffraction (XRD) analysis was carried out to determine the phases of the clay minerals. The measurements were performed on a Philips PW diffractometer (Co X-rays λ = 1.7902 Å) over the range of 5–90° 2θ for the solid powder samples. Samples were spiked with 10 wt% of zinc oxide before analysis to facilitate the calculation for the weight percent of the amorphous phase.

The morphological features and surface characteristics of samples were obtained from scanning electron microscopy (SEM) using Philips XL20 Scanning Electron Microscope at an accelerating voltage of 10 kV. The samples were coated with gold by electrodeposition under vacuum prior to analysis.

2.3. Adsorption experiment

Adsorption on the clay materials was carried out in a batch system. A desired amount of the adsorbent was added to 50 ml of known concentration of CR solution. The pH was adjusted

with 0.1 M HNO_3, and 0.1 M NaOH. The mixture was agitated at 150 rpm in a rotary shaker (Ratek OM 15 orbital mixer, Australia) at 30 °C. Due to the high CR concentration, experiments were carried out over 24 h to ensure that adsorptive equilibrium was obtained. The samples were withdrawn from the experimental flask at pre-determined time intervals until adsorption equilibrium was achieved. Then, the dye solution was separated from the adsorbent by centrifugation (Eppendorf Centrifuge 5415R, Germany) at 13,200 rpm for 20 min. The supernatants were then filtered using Millex VX filter (Millipore 0.45 μm) to ensure the solutions were free from adsorbent particles before measuring the residual dye concentration. All experiments were carried out in triplicate, and the average values were taken to minimise random error.

2.4. Analytical method

2.4.1. Dye concentration and removal capacity

Dye concentration was determined colorimetrically by measuring at maximum absorbance of 496.5 nm using a UV–visible spectrophotometer (model γ, Heλios, UK). Calibration curve was plotted between absorbance and concentration of the dye solution to obtain the absorbance-concentration profile. The percentage removal (%) of CR and amount of dye uptake per unit of adsorbent (q) were calculated using the following equations:

$$\% = (C_i - C_e) \times \frac{100}{C_i} \tag{1}$$

$$q = (C_i - C_e) \times \frac{V}{m} \tag{2}$$

where C_i is the initial dye concentration (mg l^{-1}), C_e is the dye concentration at adsorption equilibrium (mg l^{-1}), V is the volume of dye solution (ml), and m is the weight of the adsorbents (g).

2.4.2. Error analysis

Due to the inherent bias resulting from linearisation of the isotherm model, the non-linear regression Chi-square (χ^2) test was employed as a criterion for the fitting quality. This statistical analysis is based on the sum of the squares of the differences between the experimental and model calculated data, of which each squared difference was divided by the corresponding data obtained by calculating from models [18]. The Chi-square can be represented by Eq. (3).

$$\chi^2 = \sum \left[\frac{(q_{ee} - q_{ec})^2}{q_{ec}} \right] \tag{3}$$

where q_{ee} is the equilibrium capacity of the adsorbent obtained from experiment (mg g^{-1}), and q_{ec} is the calculated equilibrium capacity according to the dynamic model (mg g^{-1}). A low value of χ^2 indicates that experimental data fit better to the value from the model. In order to confirm the best-fit isotherms and kinetic models for the adsorption system, there is a need to analyse the data set using the Chi-square, combined with the values of the determined coefficient (r^2).

2.5. Theory

2.5.1. Adsorption isotherm

To simulate the adsorption isotherm, two commonly used models, the Freundlich [19] and Langmuir [20] isotherms, were selected to explicate dye–clay interaction.

2.5.1.1. Freundlich isotherm.

$$q_e = K_F C_e^{1/n} \tag{4}$$

Eq. (4) can be rearranged to obtain a linear form by taking logarithms:

$$\log q_e = \log K_F + \frac{1}{n} \log C_e \tag{5}$$

where q_e is the amount of dye adsorbed per unit of adsorbent at equilibrium (mg g^{-1}), C_e is the concentration of dye solution at equilibrium (mg l^{-1}), K_F (mg$^{1-1/n}$ $l^{1/n}$ g^{-1}) and n are the Freundlich adsorption isotherm constants, being indicative of the extent of the adsorption and the degree of nonlinearity between solution concentration and adsorption, respectively. K_F and $1/n$ values can be calculated from intercept and slope of the linear plot between $\log C_e$ and $\log q_e$.

2.5.1.2. Langmuir isotherm.

$$q_e = \frac{q_m K_L C_e}{1 + K_L C_e} \tag{6}$$

The equation can be linearised to the following equation

$$\frac{1}{q_e} = \frac{1}{q_m} + \frac{1}{K_L q_m} \frac{1}{C_e} \tag{7}$$

where q_m is the maximum amount of adsorption with complete monolayer coverage on the adsorbent surface (mg g^{-1}), and K_L is the Langmuir constant related to the energy of adsorption (l mg^{-1}). The Langmuir constants K_L and q_m can be determined from the linear plot of $1/C_e$ versus $1/q_e$.

2.5.2. Adsorption kinetics

Adsorption kinetic models were applied to interpret the experimental data to determine the controlling mechanism of dye adsorptions from aqueous solution.

2.5.2.1. Pseudo-first order model. Pseudo-first order equation or Lagergren's kinetics equation [21] is widely used for the adsorption of an adsorbate from an aqueous solution. This kinetic is based on the assumption that the rate of change of solute uptake with time is directly proportional to the difference in saturation concentration and the amount of solid uptake with time.

$$\frac{dq_t}{dt} = k_1(q_e - q_t) \tag{8}$$

when $q_t = 0$ at $t = 0$, Eq. (8) can be integrated into following equation:

$$\log(q_e - q_t) = \log q_e - \frac{k_1 t}{2.303} \tag{9}$$

where q_t is the amount of dye adsorbed per unit of adsorbent (mg g^{-1}) at time t, k_1 is the pseudo-first order rate constant (min^{-1}), and t is the contact time (min). The adsorption rate constant (k_1) were calculated from the plot of $\log(q_e - q_t)$ against t.

2.5.2.2. Pseudo-second order model. Ho and McKay [22] presented the pseudo-second order kinetic as:

$$\frac{dq_t}{dt} = k_2(q_e - q_t)^2 \tag{10}$$

Integrating Eq. (10) and noting that $q_t = 0$ at $t = 0$, the obtained equation can be rearranged into a linear form:

$$\frac{t}{q_t} = \frac{1}{k_2 q_e^2} + \frac{t}{q_e} \tag{11}$$

where k_2 is the pseudo-second order rate constant (g mg^{-1} min^{-1}). The initial adsorption rate, h (mg g^{-1} min^{-1}) at $t \to 0$ is defined as:

$$h = k_2 q_e^2 \tag{12}$$

The h, q_e and k_2 can be obtained by linear plot of t/q_t versus t.

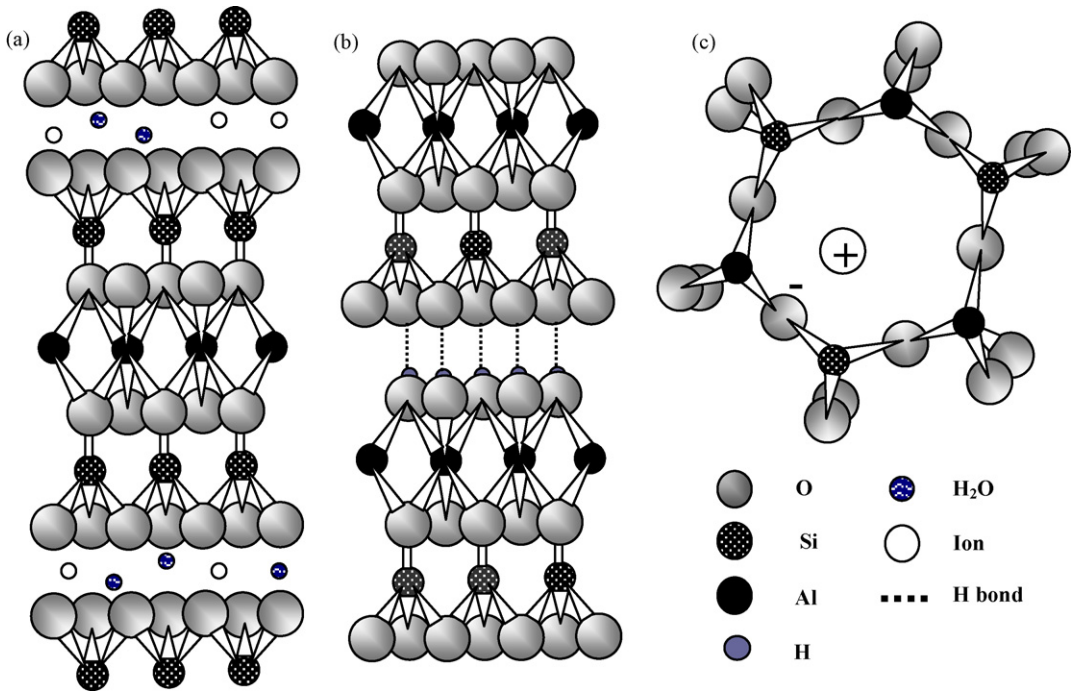

Fig. 2. The diagram of clay mineral molecular structures. (a) Bentonite (Montmorillonite), (b) Kaolinite and (c) Zeolite.

2.5.3. Adsorption mechanism

Intra-particle diffusion model is commonly used for identifying the adsorption mechanism for design purposes. The effect of intra-particle diffusion resistance on adsorption can be determined by the following relationship [23]

$$q_t = k_{id} t^{1/2} + I \quad (13)$$

where k_{id} is the intra-particle diffusion rate constant ($mg\,g^{-1}\,min^{-1/2}$). To follow the intra-particle diffusion model, a plot of q_t against $t^{1/2}$ should give a linear line where a slope is k_{id} and intercept I. Values of I give information regarding the thickness of boundary layer, i.e. the larger intercept the greater is the boundary layer effect.

3. Results and discussion

3.1. Characteristics of clay materials

3.1.1. Molecular structure

3.1.1.1. Bentonite. Bentonite is a highly colloidal and plastic clay composed mainly of a very soft montmorillonite. Special properties of bentonite are its ability to absorb large quantities of water, and form thixotrophic gels, with an accompanying increase in volume up to several times of its dry bulk. The molecular structure of bentonite is sketched in Fig. 2a. A crystalline structure of bentonite is known as 2:1 type aluminosilicate, presenting an octahedral alumina between two tetrahedral silica layers. These parallel layers are held together by weak electrostatic forces, allowing water and other polar molecules to enter between layers and induce an expansion of mineral structure [24]. Substitutions of ions of lower valence within the lattice structure, for instance, Al^{3+} for Si^{4+} in the tetrahedral sheet and Mg^{2+} for Al^{3+} in the tetrahedral layer, result in an excess of negative charge in the lattice. These imbalanced charges in the interlayer space are equalised by the dominant cations, typically Na^+, K^+, Mg^{2+}, and Ca^{2+}. These cations are exchangeable due to their loose binding, together with broken bonds with clay, attributed to a high cation exchange capacity of bentonite.

3.1.1.2. Kaolin. Kaolin or china clay is commonly referred to as clay that consists mainly of kaolinite. It is recognized as 1:1 clay as its structure presents a tetrahedral silica sheet alternating with an octahedral alumina sheet (Fig. 2b). These sheets are arranged so that the end of the silica tetrahedrons and the adjacent layers of the octahedral sheets form a layer. The layer consists of octahedral and tetrahedral groups, in which two-thirds of the oxygen atoms are allocated by the silicon and aluminium, becoming O instead of OH. The charges within the structure unit are balanced, and there is very little substitution in the interlayer space [25]. The bond held between two adjacent layers is a weak hydrogen bond, but the sum of many hydrogen bonds between units creates a strong and stable force which is nearly impossible to separate. The structure is fixed and no expansion occurs between layers when the clay is wetted. Thereby, kaolinite is defined as a nonexpanding phyllosilicate mineral.

3.1.1.3. Zeolite. Zeolite is a crystalline aluminosilicate with different cavity structures. Its molecular is structured by a three dimensional framework formed by fully connected SiO_4 and AlO_4 tetrahedra linked by coordinating oxygen atoms (Fig. 2c). An imbalance charge between Al^{3+} and four negative charges of surrounding oxygen atoms generates a negative excess charge within the lattice. This negative charge can be compensated by certain exchangeable ions in solutions, providing zeolites high ion exchange capacity. Differing from clays, zeolite is categorised as a tectosilicate (framework silicates) with microporous channels, of which their pore space is filled in a volumetric manner rather than a layer-by-layer pattern in clays [26]. The natural zeolite used in this study is a mineral of the heulandite group with high silica content. Its characteristics of tabular morphology illustrate an open reticular structure of easy access formed by open channels of 8–10 membered rings. One of the most important features of zeolites is their silicon and aluminium (Si/Al) ratio. Aluminosilicate zeolites exhibit a strongly hydrophilic capability in nature, lowering Si/Al component ratio through, i.e. acid treatment, can improve hydrophobicity on material surface and

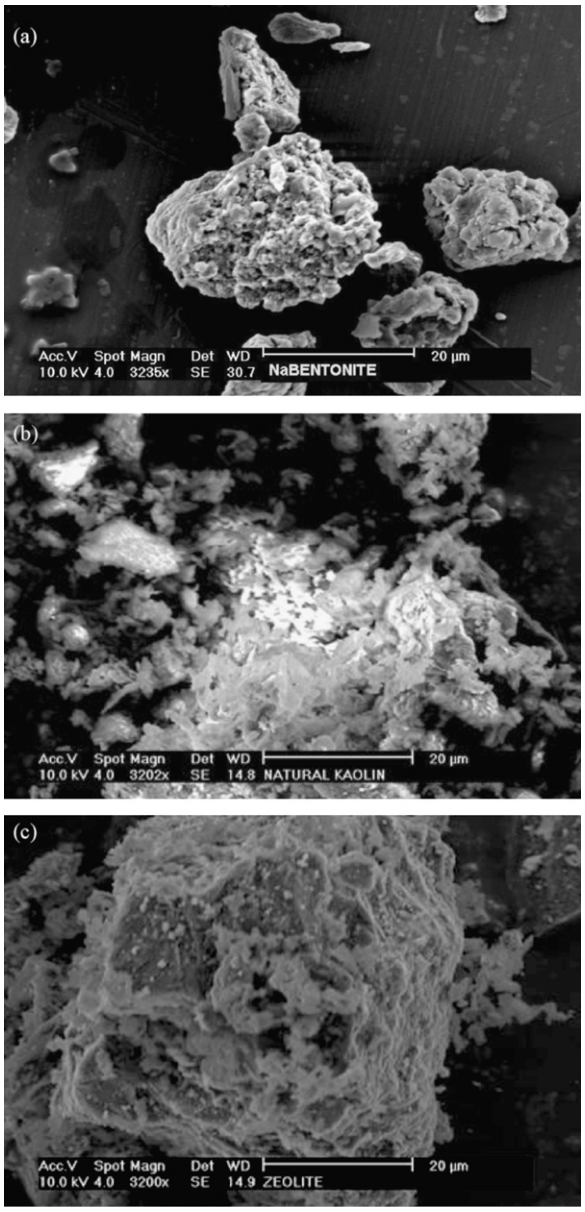

Fig. 3. Scanning electron microscopic images of clay materials. (a) Sodium bentonite, (b) Kaolin and (c) Zeolite.

increase its adsorptive favourability toward organic compounds [27].

3.1.2. Surface property

The surface morphology of these three adsorbents was observed under SEM analysis (Fig. 3). The SEM image of sodium bentonite confirms with its theoretical structure in which the soft clump and sponge like figure with consistent distribution of micropores were observed. Kaolin, on the other hand, illustrates the scattering of small solid hexagonal flakes piled up on top of one another. Zeolite shows noticeable cage-like cavities and the presence of other impurities on the surface that are generally found in untreated zeolites. The average BET surface areas of sodium bentonite, kaolin and zeolite are shown in Table 1. Bentonite has the largest specific surface area followed by kaolin.

X-ray diffraction (XRD) is the basic technique to determine the bulk structure and composition of materials with crystalline structure. From Fig. 4, XRD measurement shows that sodium bentonite is mainly composed of amorphous phase and contains less than 10% crystal phase present in the form of quartz. The majority of kaolin is reported as the crystal phase with more than 76% of the total weight. Similar crystalline content is also present in zeolite in the form of quartz, aluminite, and diaspore. Such difference in material phases can be implied to the distinctive adsorption characteristics among clays. High amorphous content and low crystal phase of sodium bentonite points out that the CR removal is rather a combination mechanisms of dye adsorption on clay surface and cation exchange between dye and foreign ions within the interlayer of the bentonite. In contrast, kaolin has a considerably lower cation exchange capacity, and performs the adsorption which is most likely to take place on the crystal surfaces and edges of clay.

3.2. Effect of dye concentration

The effect of initial CR concentration on the adsorption capacity of the clay materials was investigated under equilibrium conditions with 20 g l^{-1} of adsorbents. In Fig. 5a, a similar CR adsorption profile was observed, where the adsorption capacity increased with an increase in the dye concentration. The maximum adsorption capacity attained 5.6 mg g^{-1} for kaolin and 4.3 mg g^{-1} for zeolite in association with CR concentrations of 150 mg l^{-1} and 200 mg l^{-1}, respectively. The adsorption capacity of sodium bentonite was found to gradually reach 19.9 mg g^{-1} at 1000 mg l^{-1} of CR. The high colour removal by bentonite is corresponded to its higher specific surface area, when compared to kaolin and zeolite. It can be proposed that an increase in the initial dye concentration leads to an increase in mass gradient between the solution and adsorbent, and thus acts as a driving force for the transfer of dye molecules from bulk solution to the particle surface. The increase in the proportional dye adsorption is attributed to the equilibrium shift during the clay adsorption process [5].

3.3. Effect of adsorbent dosage

The effect of adsorbent dosage ranging from 5 to 100 g l^{-1} on the CR (150 mg l^{-1}) removal is presented in Fig. 5b. The CR removal increased as the clay dosage increased. As the adsorbent dosage increased, kaolin and zeolite demonstrated a gradual increase in CR removal from 18 to 100% and 12 to 95%, respectively. This adsorptive enhancement is ascribed to an increase in adsorption surface area of micropores and the availability of adsorption sites [17]. This investigation further confirmed that sodium bentonite demonstrated the highest adsorptive capacity. Nearly 100% CR removal was achieved using only 20 g l^{-1} of bentonite, compared to 50 g l^{-1} of kaolin and more than 100 g l^{-1} of zeolites.

3.4. Adsorption isotherm

Analysis of adsorption isotherm is of fundamental importance to describe how adsorbate molecules interact with the adsorbent surface. Equilibrium studies determine the capacity of the adsorbent and describe the adsorption isotherm by constants which values express the surface properties and affinity of the adsorbents. The relationship between equilibrium data and either theoretical or practical equations is essential for interpretation and prediction of the extent of adsorption [28]. The Freundlich isotherm was employed to describe heterogeneous systems and reversible adsorption, which does not restrict to the monolayer formations.

The favourable adsorption of the adsorption model can be determined from Freundlich constants. K_F is indicative of the adsorption capacity of the adsorbent, i.e. the greater K_F value, the greater adsorption capacity. The other Freundlich constant n is a measure

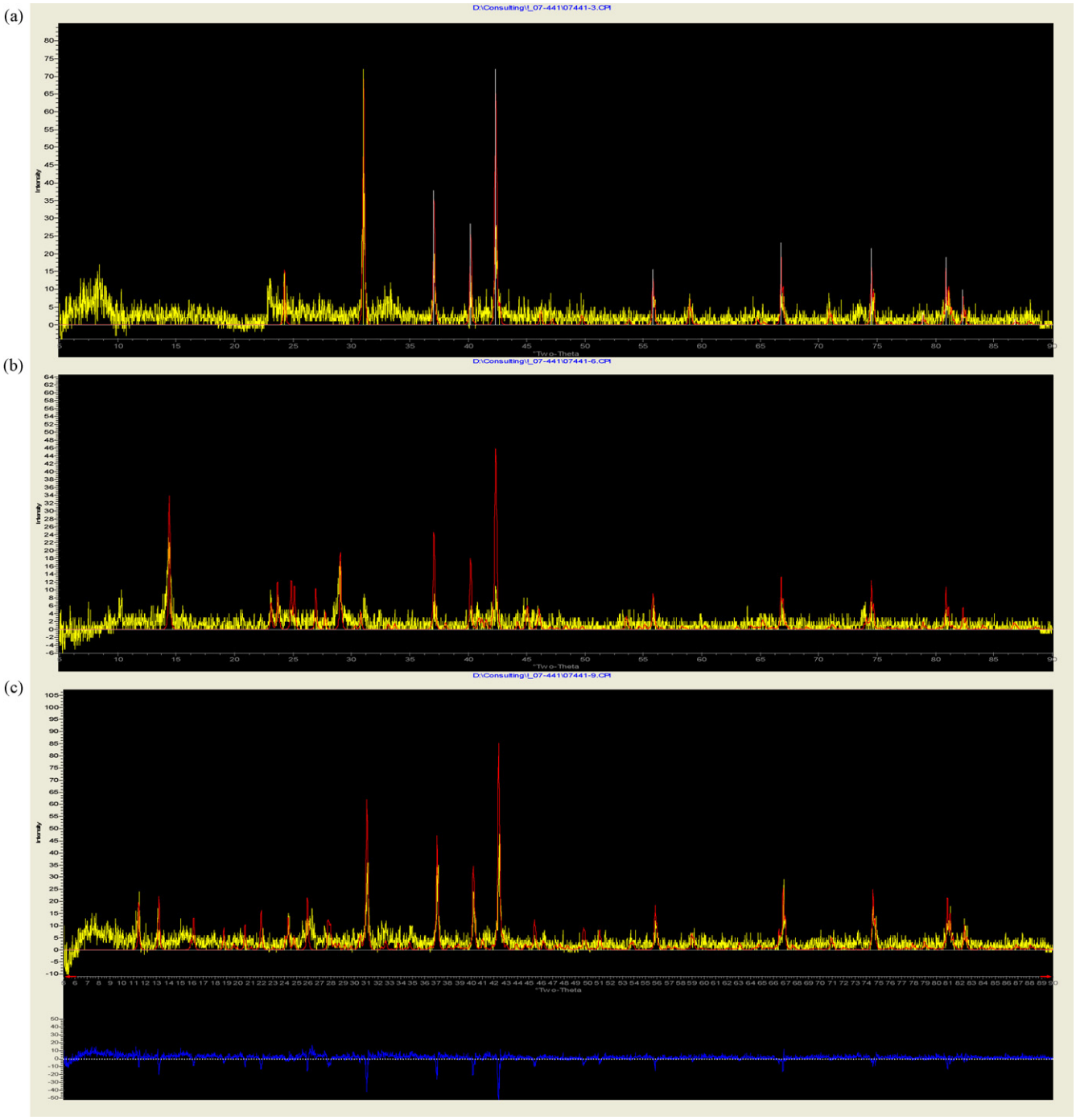

Fig. 4. X-ray diffraction patterns of Australian clay minerals. (a) Sodium bentonite, (b) Kaolin and (c) Zeolite.

of the deviation from linearity of the adsorption and used to verify types of adsorption. It is suggested that if n is equal to unity, the adsorption is linear. Furthermore, n below unity indicates that adsorption is a chemical process; whereas, n above unity is associated with a favourable adsorption and a physical process [15].

Unlike the Freundlich isotherm, the Langmuir isotherm is based on the assumption that a structure of adsorbent is homogeneous, where all sorption sites are identical and energetically equivalent. That is, each CR/clay adsorption process should have equal sorption activation energy and demonstrates the formation of monolayer coverage of dye molecule on the outer surface of clay adsorbents.

For the Langmuir model, the effect of isotherm shape is used to predict a favourability of an adsorption system under specific conditions. According to Hall et al. [29], the favourable adsorption of Langmuir isotherm can be expressed in terms of a dimensionless constant separation factor or equilibrium parameter R_L.

$$R_L = \frac{1}{1 + K_L C_i} \tag{14}$$

The values of the R_L are basically classified into four groups, indicating the shape of the isotherm as follows:

R_L	Type of isotherm
$R_L > 1$	Unfavourable
$R_L = 1$	Linear
$0 < R_L < 1$	Favourable
$R_L = 0$	Irreversible

Table 2A shows the calculated values of Freundlich and Langmuir model's parameters. The n and R_L values indicate that the CR adsorption on all clay materials is favourable for both adsorption isotherms under the experimental condition (30 °C). From Fig. 6a and b, the CR adsorption by sodium bentonite and zeolite exhibits a reasonable fit to the Langmuir model ($r^2 > 0.95$). However, a better fit to Freundlich equation was statistically confirmed by giving greater r^2 values closer to unity (0.98 and 0.99, respectively) and smaller values of χ^2. This implies that the Freundlich model may better describe an adsorption isotherm for these two adsorbents. This adsorptive behaviour indicates that the adsorption takes place on a heterogeneous surface, which may be attributed to the various active sites on sodium bentonite and zeolite having different affinities to CR molecules. The overall adsorptive performance is dominated as a physical adsorption process. The K_F values calculated from the Freundlich model (Table 2A) supported the experimental results shown in Sections 3.3 and 3.4, i.e.

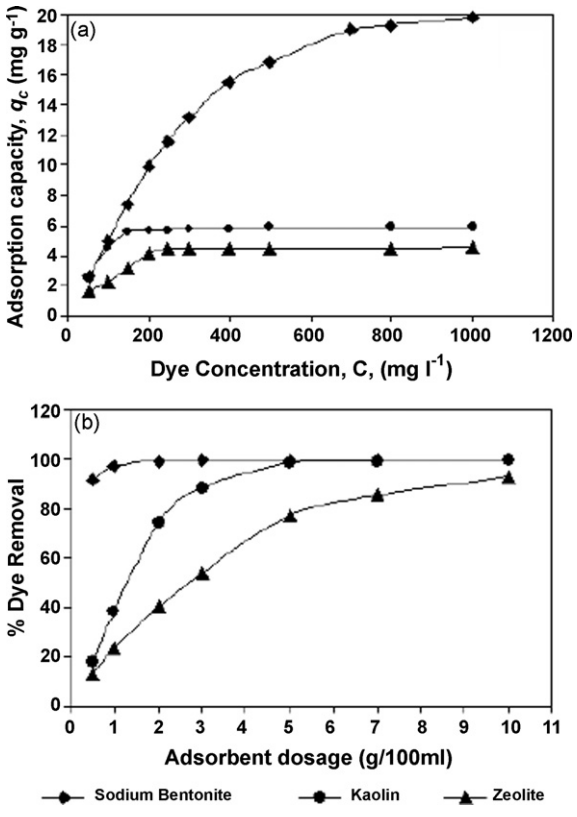

Fig. 5. Effect of (a) initial dye concentration and (b) adsorbent dosage on removal of Congo Red on Australian clay materials (adsorbent dosage 5 g, initial pH 7.5 ± 0.3).

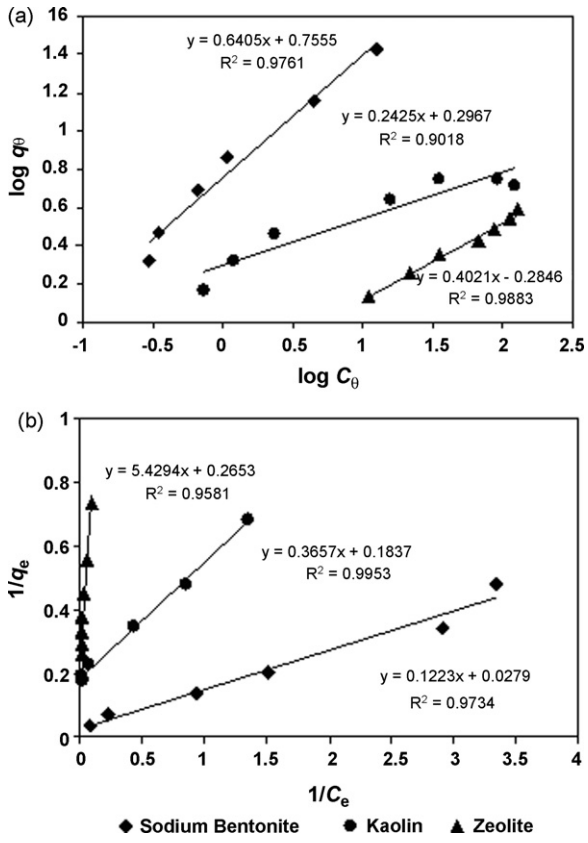

Fig. 6. Adsorption isotherm for adsorption of Congo Red on Australian clay materials (adsorbent dosage 5 g, initial dye concentration 150 mg l^{-1}, initial pH 7.5 ± 0.3) (a) Freundlich and (b) Langmuir.

bentonite has much higher adsorption capacity than kaolin and zeolite.

In contrast, the experimental data of kaolin adsorption isotherm fitted well with the Langmuir model ($r^2 > 0.99$). R_L value of the isotherm was very close to a low acceptable range, indicating a high degree of irreversibility of the adsorption process. Confirmation of experimental data into Langmuir isotherm of kaolin-CR is verified by the comparability of calculated maximum amount of monolayer adsorption (q_m) and equilibrium adsorption from experiments (q_e), showing small χ^2 given in Table 2A. The applicability of single layer coverage of dye molecules on the surface of the kaolin may be explained at the molecular level as a fact that the structure charge of kaolinite crystal is balanced and there is very little or no substitution taking place between layers. The surface area of kaolinite only equates to the external surface area and the edge surface area, where the adsorption takes place. In contrast, the adsorption with bentonite can occur between interlayer spaces.

Several studies have been investigated on removal of CR in aqueous solution using low-cost adsorbents. Table 3 summarises the adsorption capacity of different types of adsorbents for CR. It can be seen that adsorption isotherm is likely dependent on the surface properties and affinity of the adsorbents. Mesoporous activated

Table 2A
Adsorption parameter of isotherm for the adsorption of 150 mg l^{-1} Congo Red on Australian clay materials.

Materials	q_e (exp)	Freundlich				Langmuir				
		K_F	n	r^2	χ^2	K_L	R_L	q_m	r^2	χ^2
NaBentonite	7.29	5.70	1.56	0.9761	0.6048	0.23	0.03	35.84	0.9734	0.8590
Kaolin	5.58	1.98	4.12	0.9018	0.6097	0.50	0.01	5.44	0.9953	0.1022
Zeolite	3.03	0.52	2.50	0.9883	0.0300	0.05	0.12	3.77	0.9581	0.1833

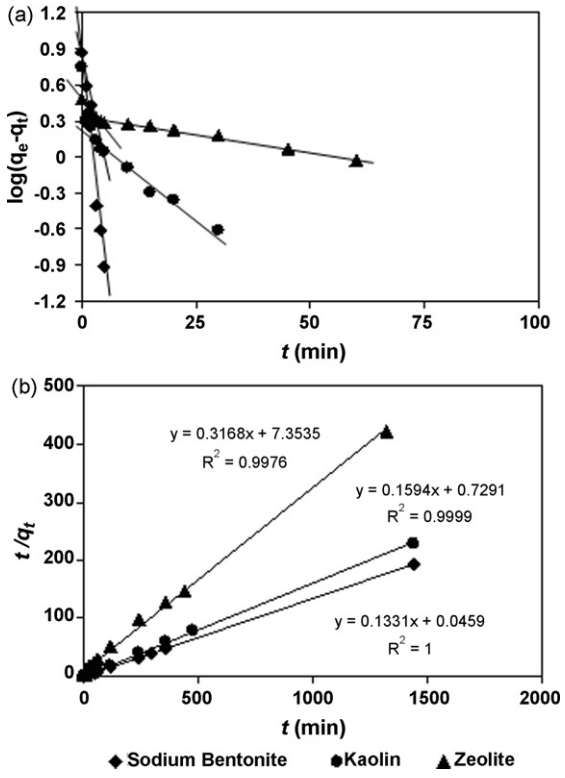

Fig. 7. Adsorption kinetic for adsorption of Congo Red on Australian clay materials (adsorbent dosage 5 g, initial dye concentration 150 mg l^{-1}, initial pH 7.5 ± 0.3) (a) Pseudo-first order and (b) Pseudo-second order.

Table 3
Adsorption isotherms of Congo Red on various adsorbents.

Adsorbent	Adsorption isotherm	q_m (mg g^{-1})	Reference
Coal-based mesoporous activated carbons	Langmuir	52–189	[28]
Chitosan hydrobeads	Langmuir	92.59	[37]
Waste orange peel	Langmuir	22.44	[6]
Bagasse fly ash	Langmuir	11.88	[17]
Activated red mud	Langmuir	7.08	[30]
Activated coir pitch carbon	Langmuir	6.72	[31]
Kaolin	Langmuir	5.44	Present study
Red mud	Langmuir	4.05	[7]
Calcium-rich fly ash	Freundlich	–	[5]
Sodium Bentonite	Freundlich	–	Present study
Zeolite	Freundlich	–	Present study

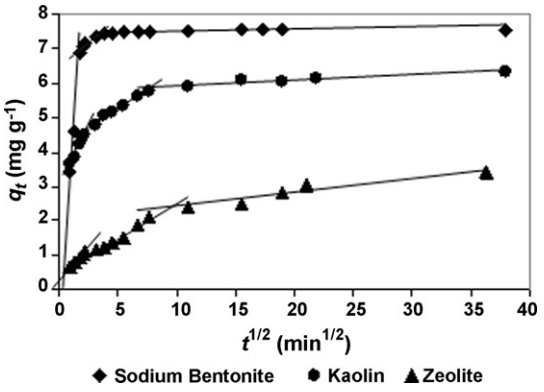

Fig. 8. Intra-particle diffusion kinetic for adsorption of Congo Red on Australian clay materials (adsorbent dosage 5 g, initial dye concentration 150 mg l^{-1}, initial pH 7.5 ± 0.3).

carbon exhibits the highest adsorption capacity in CR adsorption. This could attribute to well controlling surface properties during the material preparation. Australian clay minerals show promising potential in removal of dye when compared to untreated materials, especially when process costs are taken into account.

3.5. Adsorption kinetic

Fig. 7 presents the plots of the pseudo-first order and second order kinetics of CR adsorption on sodium bentonite, kaolin and zeolite. The calculated kinetic parameters are given in Table 2B. Fig. 7a shows that the first order kinetic curves of all adsorbents do not give a straight line but show a clear identification into several regions. This disagreement is corroborated by lower r^2 and large χ^2. As a result, it is suggested that adsorption of CR on these adsorbents did not follow pseudo-first order model in all cases.

On the contrary, the results present an ideal fit to the second order kinetic for all adsorbents with the extremely high $r^2 > 0.99$ (Fig. 7b) and very low χ^2 (Table 2B). A good agreement with this adsorption model is confirmed by the similar values of calculated q_{e2} and the experimental ones for all adsorbents; and calculated Langmuir monolayer adsorption, q_m, in the case of kaolin. The best-fit to the pseudo-second order kinetics indicates that the adsorption mechanism depends on the adsorbate and adsorbent [16], and the rate-limiting step may be chemisorption involving valence forces through sharing or exchange of electrons. Similar kinetic results have also been reported for the CR adsorption onto calcium-rich fly ash [5], xerogel [16] and coir pith carbon [31].

3.6. Adsorption mechanism

The dye sorption is usually governed by either the liquid phase mass transport rate or the intra-particle mass transport rate. Therefore, diffusive mass transfer is incorporated into the adsorption process. In this study, the Intra-particle diffusion model was applied to identify the diffusion mechanism of the CR adsorption onto the natural adsorbents. Fig. 8 shows that the adsorption plots of these natural adsorbents are not linear over the whole time range and can be separated into a few linear regions. This may reveal that there are two or three adsorption stages taking place. Lorenc-Grabowska and Gryglewicz [28] explained such multi-linearity stages that the initial portion can be attributed to external surface adsorption that the adsorbate diffuses through the solution to the external surface of the adsorbent or the boundary layer diffusion of solute molecules, where the adsorption rate is high. The second portion illustrates the gradual adsorption stage, where intra-particle diffusion rate is rate-controlling. The last portion refers to the final equilibrium

Table 2B
Adsorption parameters of kinetic for the adsorption of 150 mg l^{-1} Congo Red on Australian clay materials.

Materials	q_e (exp)	Pseudo-first order				Pseudo-second order				
		q_{e1}	k_1	r^2	χ^2	q_{e2}	h	k_2	r^2	χ^2
NaBentonite	7.29	8.77	0.16	0.9562	0.2492	7.51	21.79	0.39	1	0.0070
Kaolin	5.58	2.14	0.02	0.8959	5.4225	6.27	1.37	0.03	0.9999	0.0864
Zeolite	3.03	2.01	0.001	0.8066	0.5151	3.16	0.14	0.01	0.9976	0.0054

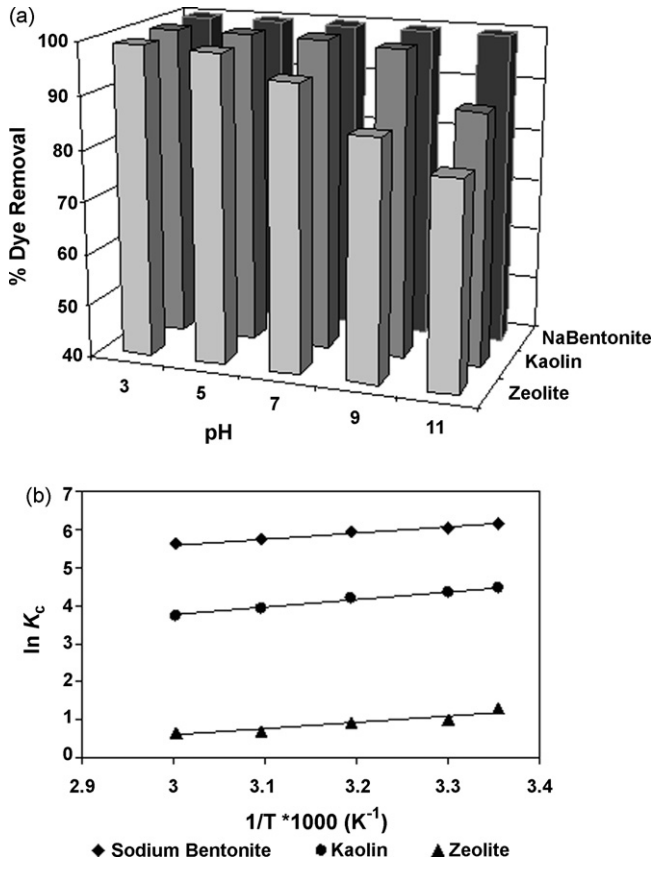

Fig. 9. Effect of (a) pH and (b) temperature on adsorption of Congo Red on Australian clay materials (adsorbent dosage 5 g, initial dye concentration 150 mg l^{-1}).

stage in which the intra-particle diffusion starts to slow down and level out as the extremely low dye concentration remains in the solution or maximum adsorption was attained. Generally, when adsorption steps are not dependent of one another; the plot of q_t against $t^{1/2}$ should give two or more intercepting lines depending on the actual mechanism [32]. The intra-particle diffusion plots of all clays provide a linear relationship; however, none of the lines passed through the origin, $I \neq 0$. This indicates that the intra-particle diffusion is involved in the adsorption process but not the only rate-controlling step. That is, some other mechanisms such as complexation or ion-exchange may also control the rate of adsorption [15,33]. The large deviation from the origin of the bentonite plot shows that the boundary layer diffusion affects the adsorption to some extent, compared to kaolin and zeolite where intercept values are smaller. Similar results have been reported in adsorption of CI reactive blue 221 on sepiolite [9] and basic dyes on Australian zeolites [34].

3.7. Effect of pH

Fig. 9a presents the effect of pH 3–11 on CR adsorption on different clay minerals. The results show that bentonite demonstrated a pH stable adsorption, whereas the adsorption by kaolin and zeolite is a pH dependent process. The adsorption capacity of zeolite decreased significantly as pH increased, while the adsorption ability of kaolin decreased when pH was higher than 9. The pH effective-adsorption can be explained by the fact that the pH of dye solution can significantly affect the surface charge of the adsorbent and the degree of ionisation and speciation of the adsorbate [15]. The reduction of dye adsorption over the pH range may relate to two possible mechanisms: electrostatic interaction and chemical reaction between clay minerals and dyes. It was reported that SiO_2, Al_2O_3 and CaO, major components of the studied adsorbents, have zero point charge values of 2.2, 8.3 and 11, respectively [17]. At an acidic pH, the negative charge of silica sites of adsorbent is counterbalanced by H^+ ions hence reducing hindrance to diffusion of dye ions [17]. Whereas, there is a significant increase in electrostatic attractions between negative charges of anionic dyes and positive charges of alumina and calcia sites, thereby increasing dye adsorption [13]. As the pH of the system increases, the number of negatively charged sites raises and the number of positively charged sites declines. A low adsorption capacity can be attributed to ionic repulsion between the clay surface and the anionic dye molecules. Besides this, an abundance of OH^- ions in basic solution creates a competitive environment with anionic ions of CR for the adsorption sites causing a decrease of adsorption.

Besides, the impact of the pH on the adsorption capacity is likely to be controlled by the properties of the absorbent and adsorbate. The different pH sensitivities given by the three clay materials may be due to the difference in molecular structure among clays (Fig. 2). The ion-exchange capacity of bentonite mostly counts on substitutions within the lattice structure. These negative charges are known to be permanent and pH independent. Whereas, the negative charges of kaolin with low isomorphous substitution are mainly derived from the broken bonds around the edges and exposed hydroxyl basal, and strongly depend upon pH [35]. On the other hand, the most significant change was observed in adsorption onto zeolites where CR is almost completely removed at pH 3 and constantly decreased to less than 80% removal at pH 11. The pH sensitivity of zeolite may also contribute to a larger content of CaO, which counts as 2.9% of total composition (0.9% and 0.1% for bentonite and zeolite, respectively). This lime can be rapidly converted into $Ca(OH)_2$ when it contacts with water. A suspension of the calcium hydroxide is a medium strength base in nature, resulting in an increasing alkalinity of the dye solution.

In addition, the noticeable increase in adsorption capacity of zeolites at the acidic pH may relate to the increased complexity of zeolite channels. Korkuna et al. [26] stated that acidic modification of natural clinoptilolite (zeolite) can improve the adsorbent characteristics due to decationation and dealumination reactions, as well as by dissolving amorphous silica fragments blocking the zeolite channels, resulting in an increase in microporous distribution. However, it was observed that at alkaline pH range, significant dye adsorption on all materials still takes place. This reveals that chemisorption might also take part in the adsorption [31]. Furthermore, it is very important to point out that more than 90% of the dye can be removed by all materials at the natural pH. This is indicative of the possibility to employ these Australian clay materials as alternative low-cost adsorbents.

3.8. Effect of temperature

Thermodynamic reaction of adsorption process can be determined via thermodynamic parameters, such as the changes in the standard free energy (ΔG°), the enthalpy (ΔH°) and entropy (ΔS°) associated with the adsorption process, using the following relation:

$$\Delta G^\circ = \Delta H^\circ - \Delta S^\circ T \quad (15)$$

$$\Delta G^\circ = -RT \ln K_C \quad (16)$$

Taking advantages of Eqs. (15) and (16), the van't Hoff equation can be written as

$$\ln K_C = \frac{\Delta S^\circ}{R} - \frac{\Delta H^\circ}{RT} \quad (17)$$

Table 4
Thermodynamic parameters for the adsorption of Congo Red on Australian clay materials at different temperatures.

Material	ΔG° (kJ mol^{-1})					ΔH° (kJ mol^{-1})	ΔS° (J mol^{-1} K^{-1})
	25 °C	30 °C	40 °C	50 °C	60 °C		
NaBentonite	−15.250	−15.240	−15.379	−15.340	−15.532	−13.021	7.411
Kaolin	−11.054	−10.989	−10.879	−10.583	−10.372	−16.968	−19.722
Zeolite	−3.194	−2.485	−2.367	−1.872	−1.857	−13.549	−35.652

where K_C is the equilibrium constant, which is the ratio of the equilibrium concentration of the dye ions on adsorbent to the equilibrium concentration of the dye ions in solution. R is the ideal gas constant (8.314 J mol^{-1} K^{-1}) and T is the adsorption temperature in Kelvin. Values of ΔG° (kJ mol^{-1}) at different temperatures were evaluated from Eq. (16). Plot of $\ln K_C$ versus $1/T$ should give a linear line, where values of ΔH° (kJ mol^{-1}) and ΔS° (J mol^{-1} K^{-1}) can be calculated from the slope and intercept of van't Hoff plots.

The results in Fig. 9b and Table 4 show the influence of temperature on adsorptive capability of the clay minerals. The adsorption of all materials is found to decrease slightly with increasing temperature from 25 to 60 °C, thereby suggesting that the adsorption process is thermodynamically stable. However, the best CR adsorption onto the studied clay minerals occurs favourably at a low temperature. This is confirmed by negative values of ΔH°, which revealed that the adsorption is exothermic and likely to be dominated by physical processes in nature involving weak forces of attraction [36]. Similar results studying CR adsorption on chitosan hydrobead where was reported by Chatterjee et al. [37], suggesting that a poor adsorption capacity at a high temperature may be attributed to the weakening of physical interaction between dye and adsorbent due to weakening of hydrogen bonds and van der Waals interaction.

In general, the change of standard free energy for physisorption is in a range of −20 to 0 kJ mol^{-1}, and the chemisorption varies between −80 and −400 kJ mol^{-1} [38]. The overall ΔG° of all adsorbents is negative values from −15.5 to −1.86 kJ mol^{-1} at the temperature range studied. These results correspond to a spontaneous physical adsorption of CR, indicating that this system does not gain energy from external resource. The shifts in magnitude of ΔG° to higher negative values of kaolin and zeolite when the temperature decreases are indicative of a rapid and more spontaneous adsorption at a low temperature [38]. The positive value of ΔS° of sodium bentonite indicates an increase in disorder of solid–liquid interface of material during adsorption of dye [39]. Conversely, the negative values ΔS° of kaolin and zeolite suggest a decrease in randomness at their solid/solution interface and no significant changes occur in the internal structure of the adsorbents through the adsorption [9].

4. Conclusions

This may be one of few studies on evaluation of naturally clay minerals, sodium bentonite, kaolin and zeolite, for removal of high dosage anionic dye from aqueous solution. SEM images and X-ray diffraction showed the different features of these adsorbents which may result in different adsorption characteristics. The Freundlich isotherm was found to be the best described adsorptive interaction for sodium bentonite and zeolite; whereas the Langmuir model was well-fitted to kaolin. Kinetic studies showed that adsorption profiles of all materials followed pseudo-second order model with multi-step diffusion process. Acidic pH condition was found to enhance the dye removal due to electrostatic attraction, but more than 90% dye removal was still obtained at neutral pH. Thermodynamic studies indicated that adsorption of all materials was stable over an extensive range of temperature. Adsorption is an exothermic reaction and can take place spontaneously in nature.

Sodium bentonite performed the best adsorption capacity (19.9 mg g^{-1}) for Congo Red removal, followed by kaolin (5.6 mg g^{-1}) and zeolite (4.3 mg g^{-1}). The high adsorption ability, less pH sensitivity and thermodynamic stability of sodium bentonite and kaolin revealed that these Australian clay minerals can be used as alternative adsorbents for removal of recalcitrant dye in industrial wastewater.

Acknowledgement

The authors are grateful to Unimin Australia Ltd and Zeolite Australia Ltd. for kindly supplying clay minerals. This work was supported by the Australian Research Council Linkage Grant (LP0562076) through the Water Environmental Biotechnology Laboratory (WEBL) at the University of Adelaide.

References

[1] P. Nigam, G. Armour, I.M. Banat, D. Singh, R. Marchant, Physical removal of textile dyes and solid state fermentation of dye adsorbed agricultural residues, Bioresour. Technol. 72 (2000) 219–226.
[2] G.M. Walker, L. Hansen, J.A. Hana, S.J. Allen, Kinetics of a reactive dye adsorption onto dolomitic sorbents, Water Res. 37 (2003) 2081–2089.
[3] M.K. Purkait, A. Maiti, S. DasGupta, S. De, Removal of congo red using activated carbon and its regeneration, J. Hazard. Mater. 145 (2007) 287–295.
[4] B.H. Hameed, A.A. Ahmad, N. Aziz, Isotherms, kinetics and thermodynamics of acid dye adsorption on activated palm ash, Chem. Eng. J. 133 (2007) 195–203.
[5] B. Acemioğlu, Adsorption of Congo red from aqueous solution onto calcium-rich fly ash, J. Colloid Interf. Sci. 274 (2004) 371–379.
[6] C. Namasivayam, N. Muniasamy, K. Gayatri, Removal of dyes from aqueous solutions by cellulostic waste orange peel, Bioresour. Technol. 57 (1996) 37–43.
[7] C. Namasivayam, D.J.S.E. Arasi, Removal of Congo Red from wastewater by adsorption onto waste red mud, Chemosphere 34 (1997) 401–417.
[8] A. Gürses, S. Karaca, C. Dogar, R. Bayrak, M. Acikyildiz, M. Yalcin, Determination of adsorptive properties of clay/water system: methylene blue sorption, J. Colloid Interf. Sci. 269 (2004) 310–314.
[9] M. Alkan, Ö. Demirbaş, M. Doğan, Adsorption kinetics and thermodynamics of an anionic dye onto sepiolite, Micropor. Mesopor. Mater. 101 (2007) 388–396.
[10] M.M. Kamel, B.M. Youssef, M.M. Kamel, Adsorption of anionic dyes by kaolinites, Dyes Pigments 15 (1991) 175–182.
[11] C.C. Wang, L.C. Juang, T.C. Hsu, C.K. Lee, J.F. Lee, F.C. Huang, Adsorption of basic dyes onto montmorillonite, J. Colloid Interf. Sci. 273 (2004) 80–86.
[12] I.K. Tonlé, E. Ngameni, H.L. Tcheumi, V. Tchiéda, C. Carteret, A. Walcarius, Sorption of methylene blue on an organoclay bearing thiol groups and application to electrochemical sensing of the dye, Talanta 74 (2008) 489–497.
[13] A.S. Özcan, B. Erdem, A. Özcan, Adsorption of Acid Blue 193 from aqueous solutions onto Na-bentonite and DTMA-bentonite, J. Colloid Interf. Sci. 280 (2004) 44–54.
[14] O. Ozdemir, B. Armagan, M. Turan, M. Celik, Comparison of the adsorption characteristics of azo-reactive dyes on mezoporous minerals, Dyes Pigments 62 (2004) 49–60.
[15] A.S. Özcan, B. Erdem, A. Özcan, Adsorption of Acid Blue 193 from aqueous solutions onto BTMA-bentonite, Colloids Surf. A: Physicochem. Eng. Aspects 266 (2005) 73–81.
[16] F. Pavan, S. Dias, E. Lima, E. Benvenutti, Removal of Congo red from aqueous solution by anilinepropylsilica xerogel, Dyes Pigments 76 (2008) 64–69.
[17] I.D. Mall, V.C. Srivastava, N.K. Agarwal, I.M. Mishra, Removal of congo red from aqueous solution by bagasse fly ash and activated carbon: Kinetic study and equilibrium isotherm analyses, Chemosphere 61 (2005) 492–501.
[18] Y.S. Ho, Selection of optimum sorption isotherm, Carbon 42 (2004) 2115–2116.
[19] H.M.F. Freundlich, Über die adsorption in lösungen, Z. Phys. Chem. 57 (1906) 385–470.
[20] I. Langmuir, The adsorption of gases on plane surfaces of glass, mica and platinum, J. Am. Chem. Soc. 40 (1918) 1361–1403.

[21] S. Lagergren, About the theory of so-called adsorption of soluble substances, Kungliga Svenska Vetenskapsakademiens, Handlingar 24 (1898) 1–39.
[22] Y.S. Ho, G. McKay, Pseudo-second order model for sorption processes, Process Biochem. 34 (1999) 451–465.
[23] W.J. Weber Jr., J.C. Morriss, Kinetics of adsorption on carbon from solution, J. Sanit. Eng. Div. Am. Soc. Civ. Eng. 89 (1963) 31–60.
[24] S. Caillere, S. Henin, Mineralogie des Argiles, Masson, Paris, 1963.
[25] R.E. Grim, Clay Mineralogy, second ed., McGraw-Hill, New York, 1968.
[26] O. Korkuna, R. Leboda, J. Skubiszewska-Zie ba, T. Vrublevs'ka, V.M. Gun'ko, J. Ryczkowski, Structural and physicochemical properties of natural zeolites: clinoptilolite and mordenite, Micropor. Mesopor. Mater. 87 (2006) 243–254.
[27] J.Y. Bottero, K. Khatib, F. Thomas, K. Jucker, J.L. Bersillon, J. Mallevialle, Adsorption of atrazine onto zeolites and organoclays in the presence of background organics, Water Res. 28 (1994) 483–490.
[28] E. Lorenc-Grabowska, G. Gryglewicz, Adsorption characteristics of Congo Red on coal-based mesoporous activated carbon, Dyes Pigments 74 (2007) 34–40.
[29] K.R. Hall, L.C. Eagleton, A. Acrivos, T. Vermeulen, Pore-and solid-diffusion kinetics in fixed-bed adsorption under constant-pattern conditions, Ind. Enq. Chem. Fundam. 5 (1966) 212–223.
[30] A. Tor, Y. Cengeloglu, Removal of congo red from aqueous solution by adsorption onto acid activated red mud, J. Hazard. Mater. B138 (2006) 409–415.
[31] C. Namasivayam, D. Kavitha, Removal of Congo Red from water by adsorption onto activated carbon prepared from coir pith, an agricultural solid waste, Dyes Pigments 54 (2002) 47–58.
[32] K. Bhattacharyya, A. Sharma, Kinetics and thermodynamics of Methylene Blue adsorption on Neem (*Azadirachta indica*) leaf powder, Dyes Pigments 66 (2005) 51–59.
[33] V.J.P. Poot, G. McKay, J.J. Healy, Removal of basic dye from effluent using wood as an adsorbent, J. Water Pollut. Control Fed. 50 (1978) 926–935.
[34] S. Wang, Z.H. Zhu, Characterisation and environmental application of an Australian natural zeolite for basic dye removal from aqueous solution, J. Hazard. Mater. B136 (2006) 946–952.
[35] C. Ma, R.A. Eggleton, Cation exchange capacity of kaolinite, Clays Clay Miner. 47 (1999) 174–180.
[36] Y. Yu, Y.Y. Zhuang, Z.H. Wang, Adsorption of water-soluble dye onto functionalized resin, J. Colloid Interf. Sci. 242 (2001) 288–293.
[37] S. Chatterjee, S. Chatterjee, B.P. Chatterjee, A.K. Guha, Adsorptive removal of congo red, a carcinogenic textile dye by chitosan hydrobeads: Binding mechanism, equilibrium and kinetics, Colloids Surf. A: Physicochem. Eng. Aspects 299 (2007) 146–152.
[38] B.S. Chu, B.S. Baharin, Y.B.C. Man, S.Y. Quek, Separation of vitamin E from palm fatty acid distillate using silica: I Equilibrium of batch adsorption, J. Food. Eng. 62 (2004) 97–103.
[39] D.G. Krishna, G. Bhattacharyya, Adsorption of methylene blue on kaolinite, Appl. Clay Sci. 20 (2002) 295–300.